Neuron
Article

Synchronous Oscillatory Neural Ensembles for Rules in the Prefrontal Cortex

Timothy J. Buschman,[1,2,3,5,6] Eric L. Denovellis,[4,5,6] Cinira Diogo,[1,3,6] Daniel Bullock,[4,5] and Earl K. Miller[1,3,5,*]
[1]The Picower Institute for Learning and Memory
[2]McGovern Institute for Brain Research
[3]Department of Brain and Cognitive Sciences
Massachusetts Institute of Technology, Cambridge, MA 02139, USA
[4]Graduate Program for Neuroscience
[5]Center for Excellence for Learning in Education, Science, and Technology
Boston University, Boston MA 02215, USA
[6]These authors contributed equally to this work
*Correspondence: ekmiller@mit.edu
http://dx.doi.org/10.1016/j.neuron.2012.09.029

SUMMARY

Intelligent behavior requires acquiring and following rules. Rules define how our behavior should fit different situations. To understand its neural mechanisms, we simultaneously recorded from multiple electrodes in dorsolateral prefrontal cortex (PFC) while monkeys switched between two rules (respond to color versus orientation). We found evidence that oscillatory synchronization of local field potentials (LFPs) formed neural ensembles representing the rules: there were rule-specific increases in synchrony at "beta" (19–40 Hz) frequencies between electrodes. In addition, individual PFC neurons synchronized to the LFP ensemble corresponding to the current rule (color versus orientation). Furthermore, the ensemble encoding the behaviorally dominant orientation rule showed increased "alpha" (6–16 Hz) synchrony when preparing to apply the alternative (weaker) color rule. This suggests that beta-frequency synchrony selects the relevant rule ensemble, while alpha-frequency synchrony deselects a stronger, but currently irrelevant, ensemble. Synchrony may act to dynamically shape task-relevant neural ensembles out of larger, overlapping circuits.

INTRODUCTION

A critical cognitive ability is the flexibility to change one's behavior based on context. Day-to-day life is full of such situations. For example, one often answers their phone when it rings but mutes it in a lecture. These context-dependent stimulus-response mappings are called "rules." By allowing us to quickly adapt to specific situations, rules endow the cognitive flexibility crucial for intelligent behavior.

The prefrontal cortex (PFC) is key to rule-based behaviors (Miller and Cohen, 2001). Rule-based tasks, especially those involving rule switching, activate the human PFC (Dove et al., 2000; MacDonald et al., 2000; Sakai and Passingham, 2003) and are impaired after PFC damage (Milner, 1963; Stuss and Benson, 1984). Many PFC neurons encode task rules (White and Wise, 1999; Wallis et al., 2001) and can "multiplex," encoding different task information (rule, stimulus, etc.) in different contexts (Rainer et al., 1999; Cromer et al., 2010). Recent theoretical work suggests that this diversity of PFC neuron properties underlies the capacity to encode a large number of diverse rules (Rigotti et al., 2010).

But this diversity raises the question of how PFC circuits satisfy two competing demands: form the neural ensembles that represent the current rule while allowing for their flexible reconfiguration when the rule changes. One proposed solution is synchronized network oscillations. Oscillations can establish ensembles of neurons in a task-dependent, flexible manner (Akam and Kullmann, 2010), allowing ensembles to be dynamically "carved" from a greater, heterogeneous population of neurons. In addition, coincident activity has a supralinear effect on downstream neurons (Aertsen et al., 1989), increasing the impact of neural ensemble activity on function (Fries, 2005).

To investigate the neural mechanisms underlying cognitive flexibility, we trained two monkeys to switch between two rules: respond to either the color or orientation of a stimulus (Figure 1A). After acquiring a central fixation target, a rule cue indicated whether the color or orientation rule was now relevant. Two different cues were used for each rule in order to disassociate neural selectivity for the cue from the rule (see Experimental Procedures). After a brief, randomized interval, a test stimulus appeared. The test stimulus consisted of small shapes that were either red or blue and were either vertically or horizontally aligned (Figure 1A). Depending on the current stimulus and rule, monkeys made a leftward or rightward saccade (color rule: red = left, blue = right; orientation rule: horizontal = left, vertical = right; Figure 1A). On most trials (70%), the color and orientation of the test stimulus signaled incongruent responses to ensure that the animals consistently followed the rule (e.g., a red/vertical cued different saccade directions under different rules). The same rule was repeated for at least 20 trials before a probabilistic switch.

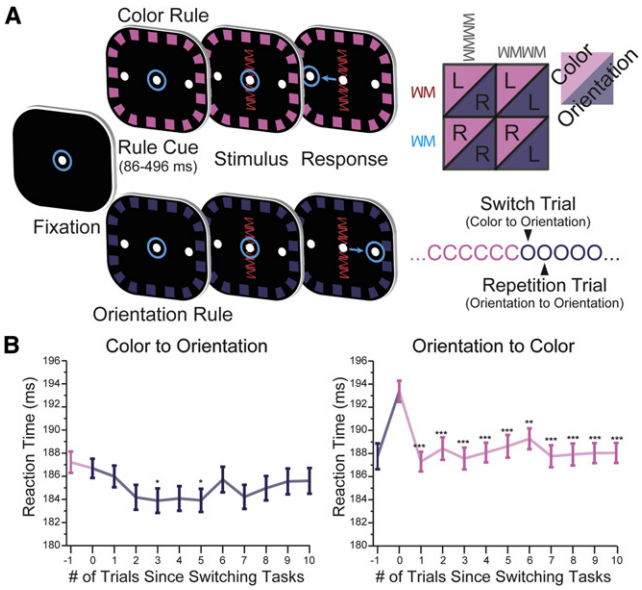

Figure 1. Task Design and Behavioral Performance

(A) Task timeline. Eye position is indicated by the blue circles. Animals initiated trial by fixating the center dot. After presentation of a border cue indicating the rule, the stimulus was presented. The animal integrated the rule and stimulus in order to make a decision about the required saccade: under the color rule, red stimuli meant saccade left and blue stimuli meant saccade right; under the orientation rule, vertical meant saccade right and horizontal meant saccade left. The rule in effect was blocked and switched randomly after a minimum of 20 trials.

(B) An asymmetric cost was observed when switching between rules, reflected in the speed at which the animals performed the task. Switching from orientation to color was significantly slower, but no cost was observed when switching from color to orientation. This suggests that orientation was behaviorally dominant. All error bars represent SEM. ***$p \leq 10^{-3}$; **$p \leq 0.01$; *$p \leq 0.05$.

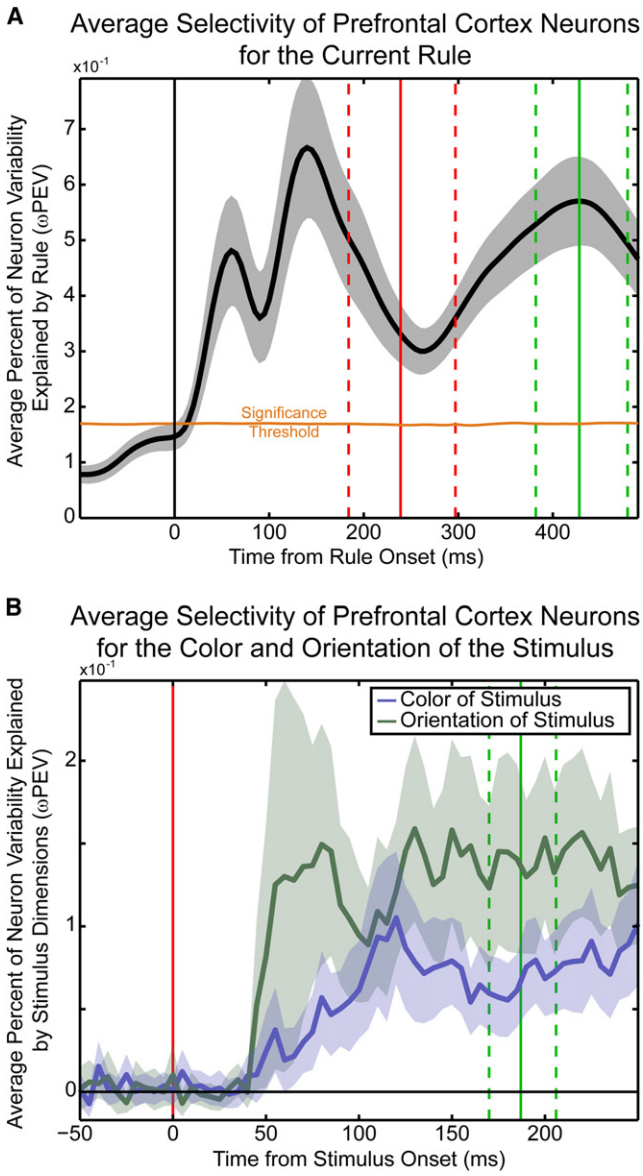

Figure 2. PFC Neurons Encode Task-Relevant Information, Including the Current Rule and Stimulus

(A) Information about the current rule (black line) is captured using a bias-corrected percent explained variance statistic (y axis) and is determined in a sliding window across the trial (x axis). Shaded region indicates 95% confidence interval. As the rule often repeated on consecutive trials (see Figure 1A), there was some expectancy of the rule encoded by PFC neurons before rule cue onset (although not significant across the population of recorded PFC neurons).

(B) PFC neurons encode stimulus identity, both its orientation (green line) and color (blue line). Shaded regions indicate 95% confidence interval. Information about the orientation of the stimulus was more strongly represented across the population, possibly leading to the behavioral dominance of the orientation rule (see Figure 1B).

RESULTS

Behavioral and Single Unit Evidence for the Dominance of the Orientation Rule

Monkeys performed well (~90% of trials were correct) but, like humans, were slower to respond on the first trial after switch, compared to repeated rule trials (Allport et al., 1994; Rogers and Monsell, 1995; Caselli and Chelazzi, 2011). This reaction time "switch cost" is thought to reflect the cognitive effort needed to change rules. However, it was only observed after a switch from orientation to color rule and not vice versa (Figure 1B; $p = 1.61 \times 10^{-4}$, generalized linear model [GLM], see Table S1 available online). This suggests that the orientation rule was behaviorally dominant, as the animals had more difficulty switching away from it.

We quantified neural information about the cued rule using a bias-corrected percent explained variance statistic (ωPEV, see Supplemental Information for details). The majority of PFC neurons carried rule information (Figure 2A, PFC: 225/313, randomization test, cluster corrected for multiple comparisons, see Figure S1A for an example neuron). Similar numbers of neurons had higher firing rates during orientation and color rule trials (108 and 117, respectively, $p = 0.25$, binomial test). Across the population of PFC neurons, rule selectivity increased after the rule cue, although some baseline rule information was

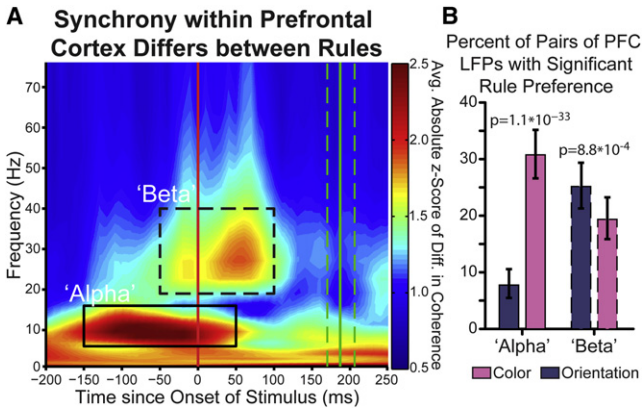

Figure 3. Rule-Selective Synchrony in PFC

(A) Synchrony between electrodes within prefrontal cortex differs for rules. Synchrony is quantified by the coherence in simultaneously recorded local field potentials during each rule. The difference in synchrony (rectified to capture synchrony differences that prefer either rule) was compared to a trial-shuffled null distribution, resulting in a *Z* score of observed rule difference (color axis). Absolute synchrony differences are shown across time relative to stimulus onset (x axis) and frequency (y axis). Two time-frequency regions of interest (ROIs) are seen—an "alpha," 6–16 Hz, prestimulus ROI (solid outline) and a "beta," 19–40 Hz, peristimulus ROI (dashed outline).

(B) Percentage of recorded pairs of electrodes with a significant rule preference during the "alpha" and "beta" time-frequency regions of interest (solid/dashed outlines in A). Error bars indicate 95% confidence interval. Significantly more electrode pairs prefer color within the alpha ROI and orientation within the beta ROI.

observed due to the task design: the rule repeated for multiple trials before a switch (Figure 2A). PFC neurons were also selective for the color or orientation of the test stimulus (104/313, 33%; 126/313, 40%, respectively). Orientation was behaviorally dominant (see above) and neural selectivity for it was more common than color ($p = 3.9 \times 10^{-3}$, binomial test), stronger across the population (Figure 2B and Figure S1C), and appeared slightly earlier (41.1 versus 47.6 ms after stimulus onset; $p = 0.0026$, permutation test).

Rule-Selective LFP Synchronization between Pairs of Electrodes

We found rule-selective oscillatory synchronization of local field potentials (LFPs) between individual PFC electrode pairs. There were significant differences in synchrony between the rules in two frequency bands during two separate trial epochs: "alpha" (6–16 Hz) after the rule cue and "beta" (19–40 Hz) after test stimulus appeared (179/465 and 207/465 recorded pairs at $p < 0.05$ in alpha and beta, respectively; Figure 3A and Figure S2A, alpha/beta shown as solid/dashed outlines). This was not due to differences in evoked potential (Figure S2E) or oscillatory power (see Supplemental Experimental Procedures). It was also not due to volume conduction of an evoked potential: many rule-selective electrode pairs were spatially interspersed with electrodes with either the opposite or no synchronous rule preference (22/79 or 28%, see Supplemental Experimental Procedures for details) and rule-selective synchrony did not monotonically decrease with distance (Figure S2C).

Beta oscillations increase with cognitive effort (Buschman and Miller, 2007; Pesaran et al., 2008; Kopell et al., 2010). Thus, we sorted electrode pairs by which rule elicited significantly stronger beta synchrony. This identified two ensembles: one synchronized during the orientation rule (n = 117 out of 465 pairs, $p < 10^{-15}$, binomial test against the number expected by chance) and one during the color rule (n = 90, $p < 10^{-15}$, binomial test). There were significantly more electrode pairs with significantly stronger beta synchrony for the orientation rule than the color rule (Figure 3B, $p = 8.8 \times 10^{-4}$), again consistent with orientation being dominant. The magnitude of rule-selective increases in synchrony were comparable to those previously observed during attention (Figures 4 and S3; Buschman and Miller, 2007; Gregoriou et al., 2009).

Rule-selective synchrony between electrodes was not between isolated electrode pairs. Rather, synchrony occurred within interconnected networks: individual electrode sites were synchronized to an average of 2.6 and 1.8 other sites for the orientation and color rule ensembles, respectively (maximum possible was 5.0, based on the number of simultaneously recorded electrodes). This degree of interconnectedness was significantly greater than expected for a random network ($p < 10^{-3}$ for both, permutation test, see Supplemental Information for details). These rule-dependent networks were highly overlapping spatially (see Figure S2D for anatomical localization of networks). The majority of recording sites that selectively increased synchrony with one set of electrodes during one rule also increased synchrony with a different set of electrodes during the other rule (58% of electrodes participating in an orientation rule-preferring pair, 52% of color rule-preferring pair, see Supplemental Information).

Task-Relevant Neurons Were Synchronized to the Current Rule Ensemble

LFP synchrony may reflect functional ensembles of spiking neurons (Fries, 2005). Indeed, we found that both stimulus- and rule-selective neurons showed rule-dependent spike LFP synchrony. When the orientation or color rule was relevant, neurons with selectivity for the relevant test stimulus modality (Figure 5A) and/or the current rule (Figure 5B) were more synchronized to the currently activated beta band color or orientation ensemble (see Supplemental Information for details). Spike-field synchrony was largely observed at beta-band frequencies, particularly for orientation rule trials (Figure 5, left column). During color rule trials, synchrony was shifted slightly toward higher frequencies (Figure 5, right column). This may reflect differences in the underlying architecture of the rule-selective ensemble either locally or between PFC and sensory and/or motor regions (Siegel et al., 2012).

Beta Orientation Ensemble Shows Stronger Alpha Color Selectivity

Alpha synchrony increases were primarily limited to color rule trials. Figure 3B shows that most of the electrode pairs that showed significant increases in synchrony in the alpha band did so when the color rule was cued. To examine this more closely, we plotted the beta synchrony-defined orientation and color ensembles separately (Figure 6). When separated, it is clear

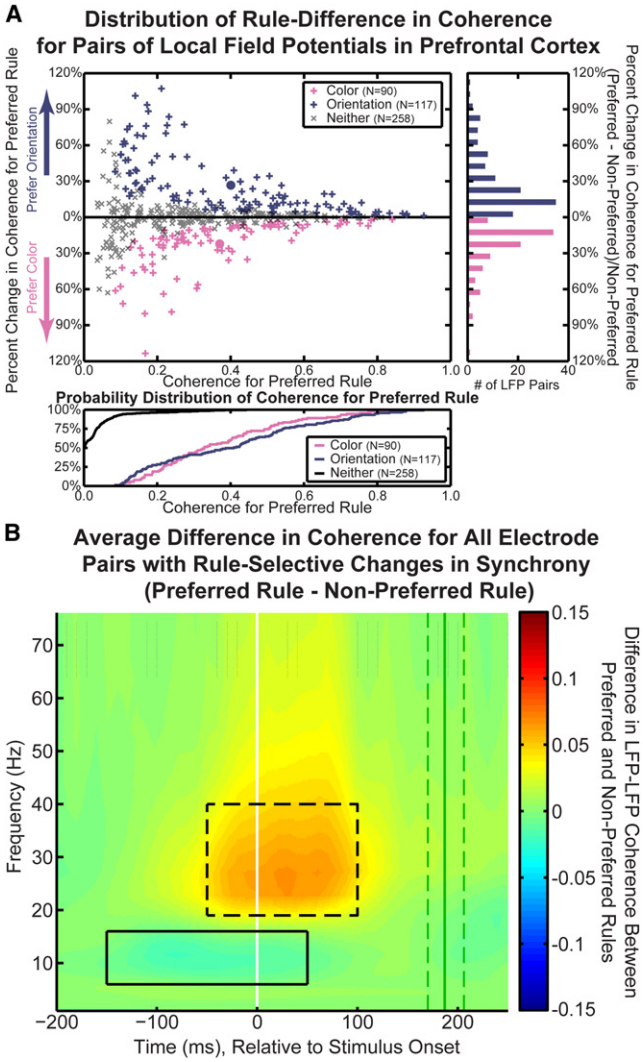

Figure 4. Magnitude of Rule-Selective Changes in Synchrony

(A) Individual electrode pairs in the beta ROI are highly synchronous and show significant rule-dependent change. Coherence between rule-dependent pairs of electrodes (pink and purple +, main panel; group averages, solid circles) in the beta ROI was high overall (cumulative probability distribution, bottom) and generally reflected a 10% or greater change in coherence over the non-preferred rule (histogram, right) compared to no-rule-preferring electrode pairs (gray x, main panel).

(B) Average difference in coherence between preferred and nonpreferred rules for all beta ROI electrode pairs.

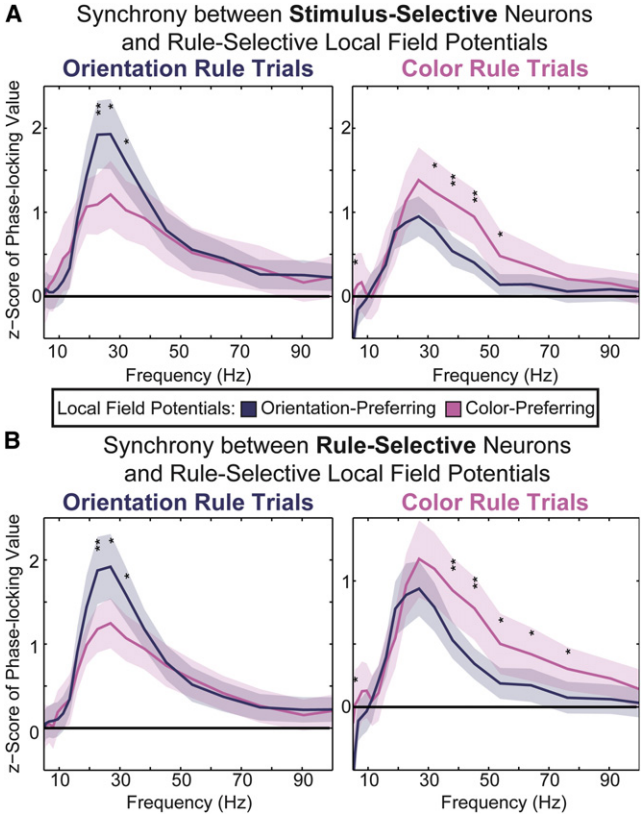

Figure 5. Single Neurons Carrying Task-Relevant Information Synchronize to the Currently Relevant Ensemble

Neurons encoding task-relevant information were more synchronized with the rule-selective ensemble preferring the current rule. Phase locking of stimulus-selective neurons (A) and rule-selective neurons (B) to electrodes that participated in either the color-preferring ensemble (pink) or the orientation-preferring ensemble (purple). Only electrodes that were exclusive to either ensemble were used (i.e., those electrodes participating in both ensembles were excluded). Phase locking is shown for both orientation trials (left) and color trials (right). Shaded regions indicate 95% confidence intervals. Significant differences in phase locking between the two ensembles are indicated at each frequency tested (*$p < 0.05$; **$p < 0.01$).

that while increases in alpha synchrony were on color trials, they were primarily limited to the orientation rule ensemble (Figure 6, left column). Indeed, electrode pairs with increased alpha synchrony during the color rule were more likely to show increased beta synchrony for the orientation rule than color rule (55/117 and 24/90 pairs, respectively; $p < 10^{-5}$, permutation test).

Synchronized alpha activity may reflect inhibition of task-irrelevant processing (Ray and Cole, 1985; Klimesch et al., 1999; Pfurtscheller, 2001; Palva and Palva, 2007; Haegens et al., 2011b). Thus, alpha synchrony during color trials may reflect "deselection" of the dominant (but currently irrelevant) orientation ensemble, allowing the weaker (but currently relevant) color ensemble to be boosted. Indeed, alpha increases in the orientation rule ensemble were associated with enhancement of individual color rule neurons. Alpha power during the preparatory interval of color trials was positively correlated with the activity level of color rule-preferring, but not orientation rule-preferring, neurons during rule application to the test stimulus (Figure S4, correlation coefficient of 0.014, $p = 0.0019$ versus 0.003, $p = 0.47$, for color and orientation rule-preferring neurons, respectively, for 100 ms after stimulus onset; color > orientation, $p = 0.047$, see Supplemental Information for details). There was no direct evidence for suppression of the orientation ensemble (e.g., a negative correlation between alpha power and the activity of orientation-preferring neurons on color trials). However, these neurons are already suppressed during the color rule, so further suppression may be harder to detect.

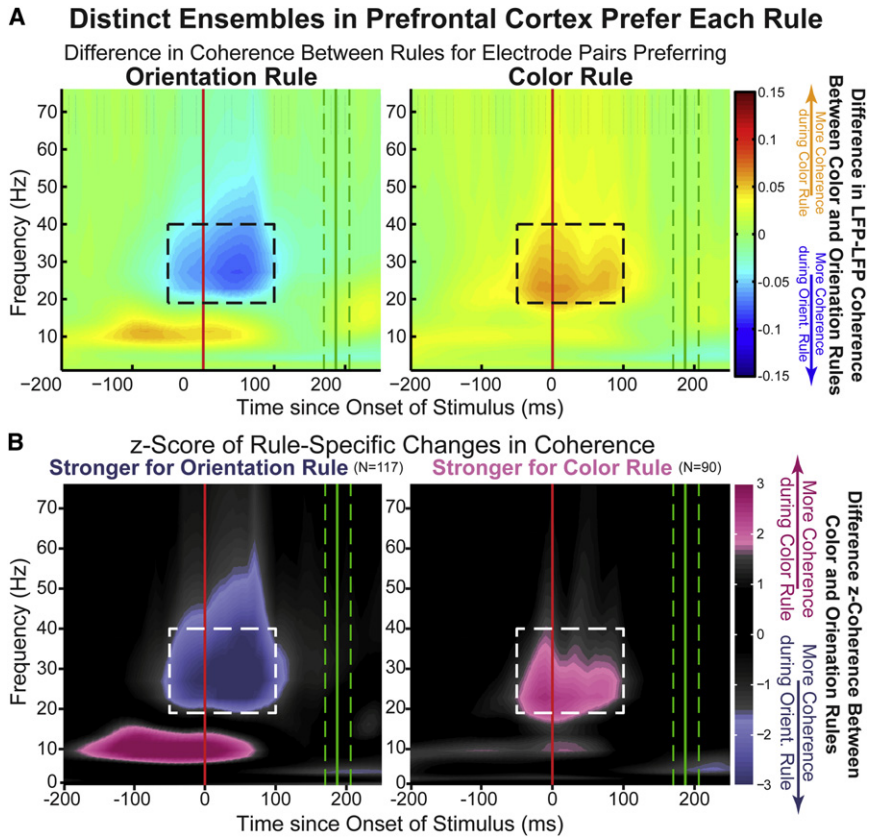

Figure 6. Independent, Rule-Specific PFC Ensembles

Ensembles within PFC can be identified by rule-selective synchrony in the peristimulus "beta" ROI (dashed outline). One ensemble is more synchronous during orientation trials (A, left). This difference is significantly greater than expected by chance (B, left). A separate ensemble of electrodes is more synchronous during color trials (A, right). Again, this difference is significant (B, right). Alpha-band synchrony is observed in the orientation ensemble during the competing color rule (left panels, orange and pink colors for top and bottom rows) but not in the color ensemble (right) or during the orientation rule (Figure 2B). Axes are the same as Figure 3A, but now color axes are no longer rectified: orange (top row) and pink (bottom row) reflect greater synchrony during color rule trials; blue (top row) and purple (bottom row) during orientation rule trials. Please note the color axis of (B) is intentionally nonlinear, showing only significant rule selectivity, beginning at a Z score of ±1.67 ($p = 0.05$) and fully saturated at ±1.97 ($p = 0.01$).

Rule-Dependent Synchrony Correlates with Behavioral Reaction Time

Synchrony at both alpha and beta was correlated with behavioral reaction time, further suggesting their functional role. There was significantly stronger rule-selective synchrony in both bands on trials with shorter reaction times (Figure 7; alpha: $p = 3.43 \times 10^{-10}$, beta: $p = 2.71 \times 10^{-3}$, Wilcoxon signed-rank test), even after controlling for the effects of preparatory time and rule on reaction time (see Table S1). This stronger synchrony with faster reaction times occurred prior to test stimulus for both alpha and beta (Figure 7; stronger selectivity in beta: −20 to 0 ms, alpha: −240 to 0 ms prior to stimulus onset, Wilcoxon signed-rank test, $p < 0.05$, Bonferroni correction), suggesting preparatory facilitation of test stimulus processing.

DISCUSSION

Linking Task-Relevant Neurons with Rule-Dependent Synchrony

Our results suggest distinct synchronous PFC ensembles support different rules. Rule-selective beta-band synchrony may help to dynamically link neurons in order to support task performance. Indeed, task-relevant (rule- and stimulus-selective) neurons were more synchronized to the corresponding ensemble for the current rule. Similar organization of neural activity by synchronous population oscillations have been seen during sensory processing (Lakatos et al., 2008) and attention (Buschman and Miller, 2009). This synchrony-based linking of neurons into ensembles could be an ideal mechanism for cognitive flexibility, allowing ensembles of task-relevant neurons to be dynamically formed and reformed (Sejnowski and Paulsen, 2006; Womelsdorf et al., 2007).

Our results are consistent with recent evidence from humans and monkeys suggesting that beta oscillations play a major role in top-down organization of neural processing (Engel and Fries, 2010; Oswal et al., 2012). There is enhancement of beta oscillations in human sensorimotor cortices when maintaining posture (Gilbertson et al., 2005; Androulidakis et al., 2007) and when competing movements need to be inhibited (Pfurtscheller, 1981; Swann et al., 2009). Beta synchronization between frontal and parietal cortices increases during top-down attention (Gross et al., 2006; Buschman and Miller, 2007, 2009) and with increased working memory load (Babiloni et al., 2004; Axmacher et al., 2008). Further, beta synchronization increases in anticipation of an upcoming stimulus and is stronger when a stimulus is more predictable (Liang et al., 2002; Gross et al., 2006; Zhang et al., 2008). Similarly, we observed that rule-selective beta synchronization in anticipation of the test stimulus was correlated with the animal's reaction time.

Coordination of Neural Ensembles

Orientation seemed to be the dominant modality. This may be due to its relative saliency, much like word naming in the Stroop test (MacLeod, 1991). We found the orientation ensemble, which was synchronized at beta-band frequencies during the orientation rule, had increased alpha-band synchrony when color was relevant. Recent studies in humans have suggested a role for alpha oscillations in working memory (Jensen et al., 2002; Freunberger et al., 2008; Palva et al., 2011) and visual attention (von Stein et al., 2000; Sauseng et al., 2005; Sadaghiani et al.,

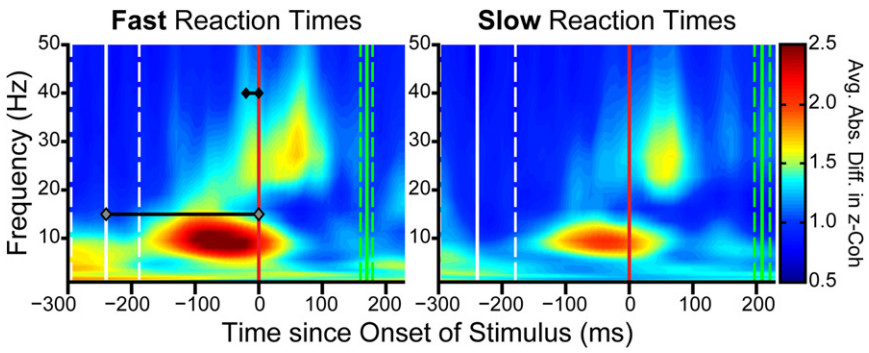

Figure 7. Strength of Prefrontal Synchrony Selectivity Correlates with Reaction Time
Trials in which the monkeys responded faster (left) showed stronger rule-selective synchrony in the "alpha" and "beta" regions of interest compared to trials with slower reaction times (right). Green lines indicate reaction time quartiles and white lines indicate the corresponding preparatory period quartiles. Black lines on faster reaction time trials (left) indicate when synchrony in the alpha- and beta-frequency bands (gray and black diamonds, respectively) was significantly higher than synchrony during slower-reaction time trials.

2010). In particular, alpha oscillations during attention are suppressed in the task-relevant sensorimotor cortices, enhanced in the task-irrelevant cortices, and can influence discriminability of stimuli (Worden et al., 2000; Gould et al., 2011; Haegens et al., 2011a). Because of this, it has been suggested that enhanced alpha synchronization creates an inhibition of irrelevant processes (Klimesch et al., 2007; Mathewson et al., 2011). Our study is consistent with this model: alpha synchronization may allow the weaker color ensemble to be activated over the stronger (orientation) ensemble when color is relevant. In support, we observed an increase in the activity of color-selective neurons after an increase in alpha in the orientation ensemble. These results suggest a dual model of competition between ensembles of neurons: beta synchrony selects the relevant ensemble, while alpha may deselect the irrelevant, but dominant, ensemble so that a weaker, relevant one can be established. Similar dual mechanisms may bias competition between stimuli during focal attention, leading to high-frequency synchronization of neural activity representing attended stimuli (Fries et al., 2001) and slower-frequency synchronization of neural activity representing unattended stimuli (Cohen and Maunsell, 2009; Mitchell et al., 2009).

In sum, our results suggest that synchronous oscillations allow dynamic selection of currently relevant neural ensembles. This may be particularly important in prefrontal cortex, where neurons have highly diverse properties and thus a particular ensemble must be formed from neurons that are also members of other ensembles (Rigotti et al., 2010). The dynamic nature of synchronized oscillations may provide a substrate for the ensembles that allows their rapid selection and deselection and, hence, cognitive flexibility.

EXPERIMENTAL PROCEDURES

Recording Locations and Techniques

Two macaque monkeys, one male (CC, *Macaca fascicularis*) and one female (ISA, *Macaca mulatta*), were trained on a cued task-switching paradigm (Figure 1A). Neural activity was simultaneously recorded during task performance from two frontal regions: the dorsolateral prefrontal cortex (PFC, area 9/46) and the anterior cingulate cortex (ACC, areas 24c and 32). Only data from the dorsolateral prefrontal cortex are reported here. The recording well targeting PFC was placed in the left hemisphere and was centered approximately 28 mm anterior to the interaural plane and 21 mm lateral from the midline. Stereotaxic positioning of the well was guided by structural magnetic resonance imaging.

Neural activity was recorded during 34 sessions (11 for monkey CC, 23 for monkey ISA). Arrays of up to sixteen epoxy-coated tungsten electrodes (FHC) were lowered into the PFC during each recording session (median number of electrodes with well-isolated single neuron activity was 5.5 per session). Electrodes were lowered in pairs by a custom-built microdrive assembly and spaced at least 1 mm apart. Electrodes were lowered acutely each day through an intact dura and allowed to settle before recording. This ensured stable isolation of the single neuron activity. After each recording session, the electrodes were retracted and the microdrive assembly was removed from the well.

A Plexon Multichannel Acquisition Processor (MAP; Plexon) was used to perform electrophysiological recordings. The signal from each electrode was filtered by the preamplifier between 154 Hz and 8.8 kHz to isolate spiking activity and between 3.3 and 88 Hz to isolate the local field potential. Both spiking activity and local field potentials were referenced to earth ground (although the same results were observed when rereferencing locally, within PFC). The raw spiking waveforms were digitized at 40 kHz and subsequently sorted into single units offline, based on waveform shape characteristics and principal components analysis (Offline Sorter, Plexon). During recording, electrodes were lowered to maximize the signal-to-noise ratio of spiking activity and were not guided by the task relevance of neural responses. This ensured a representative sample of neural activity without selection bias. A total of 313 neurons were recorded in the PFC (99 in monkey CC and 214 in monkey ISA). The average firing rate of neurons recorded in PFC was 7.4 Hz (interquartile range of firing rate was 1.7 to 10.1 Hz). Only local field potentials from electrodes with at least one isolated unit were used for all of our analyses, ensuring the electrode was in the appropriate cell layer.

Animal eye position was monitored using an infrared eye-tracking system (Eyelink, SR Research), which sampled the eye position at 240 Hz. Behavioral control was handled by Cortex (http://www.cortex.salk.edu). Animal procedures followed all guidelines set by the Massachusetts Institute of Technology Committee on Animal Care and the National Institutes of Health. Code used in the analysis was custom written in MATLAB (MathWorks) or R (R Foundation for Statistical Computing).

Behavioral Task

The task began with the presentation of a fixation spot at the center of the screen. The monkeys were required to acquire and maintain fixation within three degrees of this spot until making a behavioral response. Immediately after fixation was acquired, both the rule cue and response targets appeared and remained on screen for the duration of the trial. The rule cue was a colored border around the display indicating the feature of the stimulus the monkey needed to discriminate on the current trial. The animals were trained to perform two different rules: color and orientation. Each rule was associated with two different cues in order to distinguish rule-related activity from cue-related activity (see Figure S1A for example neurons encoding the rule and not the individual cues). After the presentation of the rule cue, the animals were required to maintain fixation for a "preparatory" time period before the onset of the stimulus. The duration of the preparatory period was randomized for each monkey (227–496 ms for monkey CC, 86–367 ms for monkey ISA; different ranges were the result of iteratively lowering the preparatory period during training while equalizing performance between animals).

At the end of the preparatory period, a test stimulus, oriented either vertically or horizontally and colored either red or blue, appeared at the center of the

screen. The test stimulus consisted of small shapes (colored and aligned appropriately). The identity of these small items changed from session to session, ensuring the animals generalized the rules. After the onset of the stimulus, the monkeys were free to make their response: a single saccade to either the left or right target. The correct saccade direction depended on both the stimulus identity and the current rule in effect (Figure 1A). For the color rule, a red stimulus required a saccade to the right, and a blue stimulus a saccade to the left. For the orientation rule, a horizontal stimulus required a saccade to the right, and a vertical stimulus a saccade to the left. As each stimulus consisted of both an orientation and color dimension, the correct saccade for the two rules could be either the same (congruent trials) or different (incongruent trials). For example, a red vertical stimulus is incongruent, requiring a rightward saccade under the color rule and a leftward saccade under the orientation rule. In contrast, a red horizontal stimulus requires a rightward saccade for both rules. The majority (70%) of trials were incongruent, ensuring the animal always followed the rule. After the animal made the correct saccade, a juice reward was delivered via a juice tube. There was an intertrial interval of approximately 100 ms before the next trial began.

Although the rule was cued on each trial, the rule in effect was blocked into groups of trials. Each block consisted of a minimum of 20 trials of the same rule. After 20 trials, the rule switched randomly—with a 5% or 10% chance of switching rules on each trial for monkey ISA and CC, respectively. The average block consisted of 39 trials of the same rule for ISA and 30 for CC.

Behavioral and Neural Analysis Methods

A generalized linear model (GLM) was used to quantify the effect of multiple task-related covariates on the animals' behavioral reaction time. A gamma distribution was used in the model, as it is ideal for fitting strictly positive data with a constant coefficient of variation, such as reaction times (McCullagh and Nelder, 1989). The link function, which defines a nonlinear transformation between the linear predictors and the mean of the observations, was chosen to be the log function to enforce the requirement that reaction times be strictly positive. A complete model was developed, fitting the reaction time with all task-related covariates: the rule (color/orientation), preparatory period, congruency of stimulus-response association across rules, monkeys, time in session, and whether it was a switch trial (see Supplemental Information for details).

A bias-corrected percent explained variance statistic (ωPEV) was used to evaluate neural selectivity. ωPEV determines the portion of variance of a neuron's firing rate explained by a particular task variable (e.g., the current rule) but is analytically corrected for upward bias in percent explained variance with limited observations. Significance was determined by a permutation procedure (see Supplemental Information for details).

Synchrony Analysis Methods

The LFP was transformed into the time-frequency domain using Morlet wavelets. Synchrony was estimated by computing the spectral coherence between pairs of electrodes. Significant differences in coherence between the two rules were determined with a permutation test. The null hypothesis is that no significant difference exists between rules, therefore a null distribution was generated by permuting color and orientation trials and recalculating the coherence (this process was repeated at least 100 times for each pair of electrodes). The mean and variance of this null distribution was used to estimate the likelihood of the observed synchrony (captured by a Z score statistic). Z scores greater than 1.96 or -1.96 indicated significant changes in coherence for the color and orientation rule, respectively (see Supplemental Information for details). Time-frequency regions of interest (e.g., the "alpha" and "beta" bands) were defined such that they encapsulated the peaks in rule-selective changes in synchrony (Figures 2 and S3). Although the bands were not predefined, they closely follow the alpha and beta bands defined in other studies, supporting conclusions about common mechanisms (see Discussion).

Phase-locking value (PLV) was used to estimate spike-field synchrony. The phase locking of task-relevant neurons (as identified by ωPEV, see above) to the LFP of electrodes participating in either the color or orientation network was estimated in a 200 ms window around the time of stimulus onset (-50 ms to 150 ms). In order to correct for the strong sample size bias in estimating spike-field synchrony, a stratification procedure was used (requiring 200 spikes in the window). Significant differences were determined by a permutation test, as above (see Supplemental Information for details).

The relationship between rule-dependent LFP synchrony and reaction time was determined by first regressing out the effect of preparation time on reaction time (see Supplemental Information for details). The resulting reaction time residuals were sorted into "fast" and "slow" trials (defined as the 65th–95th and 5th–35th percentile of the residual distribution for each session, respectively). As above, a permutation test was used to estimate a Z score of the observed rule-selective differences in synchrony (see Supplemental Information for details). Significant differences in rule selectivity between fast and slow trials were determined by comparing the average absolute Z score in the beta (or alpha)-frequency bands using a Wilcoxon signed-rank test. To preclude dependence between electrodes recorded in the same session, we bootstrap resampled the electrode pairs 1,000 times. After establishing that rule selectivity was stronger on average in the alpha and beta bands, respectively, we examined rule selectivity for differences over time by testing for differences in rule selectivity at each time point, again using a Wilcoxon signed-rank test (see Supplemental Information for further details).

SUPPLEMENTAL INFORMATION

Supplemental Information includes four figures, one table, and Supplemental Experimental Procedures and can be found with this article online at http://dx.doi.org/10.1016/j.neuron.2012.09.029.

ACKNOWLEDGMENTS

This work was supported by NSF CELEST grant GC-208001NGA and National Institute of Mental Health grant P50-MH058880. We thank S. Henrickson, S.W. Michalka, and M. Wicherski for comments on the manuscript and W. Asaad, J. Roy, and M. Siegel for technical support. E.K.M. conceived of and designed the experiment; C.D. designed the experiment, trained monkeys, and collected neural data; and T.J.B. and E.L.D. conceived of, implemented, and executed data analysis; T.J.B., E.L.D., D.B., and E.K.M. wrote the manuscript.

Accepted: September 19, 2012
Published: November 21, 2012

REFERENCES

Aertsen, A.M., Gerstein, G.L., Habib, M.K., and Palm, G. (1989). Dynamics of neuronal firing correlation: modulation of "effective connectivity". J. Neurophysiol. *61*, 900–917.

Akam, T., and Kullmann, D.M. (2010). Oscillations and filtering networks support flexible routing of information. Neuron *67*, 308–320.

Allport, D.A., Styles, E.A., and Hsieh, S. (1994). Shifting intentional set: Exploring the dynamic control of tasks. In Attention and Performance XV: Conscious and Nonconscious Information Processing, C. Umilta and M. Moscovitch, eds. (Cambridge, MA: The MIT Press), pp. 421–452.

Androulidakis, A.G., Doyle, L.M.F., Yarrow, K., Litvak, V., Gilbertson, T.P., and Brown, P. (2007). Anticipatory changes in beta synchrony in the human corticospinal system and associated improvements in task performance. Eur. J. Neurosci. *25*, 3758–3765.

Axmacher, N., Schmitz, D.P., Wagner, T., Elger, C.E., and Fell, J. (2008). Interactions between medial temporal lobe, prefrontal cortex, and inferior temporal regions during visual working memory: a combined intracranial EEG and functional magnetic resonance imaging study. J. Neurosci. *28*, 7304–7312.

Babiloni, C., Babiloni, F., Carducci, F., Cincotti, F., Vecchio, F., Cola, B., Rossi, S., Miniussi, C., and Rossini, P.M. (2004). Functional frontoparietal connectivity during short-term memory as revealed by high-resolution EEG coherence analysis. Behav. Neurosci. *118*, 687–697.

Buschman, T.J., and Miller, E.K. (2007). Top-down versus bottom-up control of attention in the prefrontal and posterior parietal cortices. Science *315*, 1860–1862.

Buschman, T.J., and Miller, E.K. (2009). Serial, covert shifts of attention during visual search are reflected by the frontal eye fields and correlated with population oscillations. Neuron *63*, 386–396.

Caselli, L., and Chelazzi, L. (2011). Does the macaque monkey provide a good model for studying human executive control? A comparative behavioral study of task switching. PLoS ONE *6*, e21489.

Cohen, M.R., and Maunsell, J.H.R. (2009). Attention improves performance primarily by reducing interneuronal correlations. Nat. Neurosci. *12*, 1594–1600.

Cromer, J.A., Roy, J.E., and Miller, E.K. (2010). Representation of multiple, independent categories in the primate prefrontal cortex. Neuron *66*, 796–807.

Dove, A., Pollmann, S., Schubert, T., Wiggins, C.J., and von Cramon, D.Y. (2000). Prefrontal cortex activation in task switching: an event-related fMRI study. Brain Res. Cogn. Brain Res. *9*, 103–109.

Engel, A.K., and Fries, P. (2010). Beta-band oscillations—signalling the status quo? Curr. Opin. Neurobiol. *20*, 156–165.

Freunberger, R., Klimesch, W., Griesmayr, B., Sauseng, P., and Gruber, W. (2008). Alpha phase coupling reflects object recognition. Neuroimage *42*, 928–935.

Fries, P. (2005). A mechanism for cognitive dynamics: neuronal communication through neuronal coherence. Trends Cogn. Sci. *9*, 474–480.

Fries, P., Reynolds, J.H., Rorie, A.E., and Desimone, R. (2001). Modulation of oscillatory neuronal synchronization by selective visual attention. Science *291*, 1560–1563.

Gilbertson, T., Lalo, E., Doyle, L., Di Lazzaro, V., Cioni, B., and Brown, P. (2005). Existing motor state is favored at the expense of new movement during 13-35 Hz oscillatory synchrony in the human corticospinal system. J. Neurosci. *25*, 7771–7779.

Gould, I.C., Rushworth, M.F., and Nobre, A.C. (2011). Indexing the graded allocation of visuospatial attention using anticipatory alpha oscillations. J. Neurophysiol. *105*, 1318–1326.

Gregoriou, G.G., Gotts, S.J., Zhou, H., and Desimone, R. (2009). High-frequency, long-range coupling between prefrontal and visual cortex during attention. Science *324*, 1207–1210.

Gross, J., Schmitz, F., Schnitzler, I., Kessler, K., Shapiro, K., Hommel, B., and Schnitzler, A. (2006). Anticipatory control of long-range phase synchronization. Eur. J. Neurosci. *24*, 2057–2060.

Haegens, S., Händel, B.F., and Jensen, O. (2011a). Top-down controlled alpha band activity in somatosensory areas determines behavioral performance in a discrimination task. J. Neurosci. *31*, 5197–5204.

Haegens, S., Nácher, V., Luna, R., Romo, R., and Jensen, O. (2011b). α-Oscillations in the monkey sensorimotor network influence discrimination performance by rhythmical inhibition of neuronal spiking. Proc. Natl. Acad. Sci. USA *108*, 19377–19382.

Jensen, O., Gelfand, J., Kounios, J., and Lisman, J.E. (2002). Oscillations in the alpha band (9-12 Hz) increase with memory load during retention in a short-term memory task. Cereb. Cortex *12*, 877–882.

Klimesch, W., Doppelmayr, M., Schwaiger, J., Auinger, P., and Winkler, T. (1999). 'Paradoxical' alpha synchronization in a memory task. Brain Res. Cogn. Brain Res. *7*, 493–501.

Klimesch, W., Sauseng, P., and Hanslmayr, S. (2007). EEG alpha oscillations: the inhibition-timing hypothesis. Brain Res. Brain Res. Rev. *53*, 63–88.

Kopell, N., Kramer, M.A., Malerba, P., and Whittington, M.A. (2010). Are different rhythms good for different functions? Front Hum Neurosci. *4*, 187.

Lakatos, P., Karmos, G., Mehta, A.D., Ulbert, I., and Schroeder, C.E. (2008). Entrainment of neuronal oscillations as a mechanism of attentional selection. Science *320*, 110–113.

Liang, H., Bressler, S.L., Ding, M., Truccolo, W.A., and Nakamura, R. (2002). Synchronized activity in prefrontal cortex during anticipation of visuomotor processing. Neuroreport *13*, 2011–2015.

MacDonald, A.W., 3rd, Cohen, J.D., Stenger, V.A., and Carter, C.S. (2000). Dissociating the role of the dorsolateral prefrontal and anterior cingulate cortex in cognitive control. Science *288*, 1835–1838.

MacLeod, C.M. (1991). Half a century of research on the Stroop effect: an integrative review. Psychol. Bull. *109*, 163–203.

Mathewson, K.E., Lleras, A., Beck, D.M., Fabiani, M., Ro, T., and Gratton, G. (2011). Pulsed out of awareness: EEG alpha oscillations represent a pulsed-inhibition of ongoing cortical processing. Front Psychol *2*, 99.

McCullagh, P., and Nelder, J.A. (1989). Generalized Linear Models (Boca Raton, FL: Chapman & Hall/CRC).

Miller, E.K., and Cohen, J.D. (2001). An integrative theory of prefrontal cortex function. Annu. Rev. Neurosci. *24*, 167–202.

Milner, B. (1963). Effects of different brain lesions on card sorting: The role of the frontal lobes. Arch. Neurol. *9*, 90.

Mitchell, J.F., Sundberg, K.A., and Reynolds, J.H. (2009). Spatial attention decorrelates intrinsic activity fluctuations in macaque area V4. Neuron *63*, 879–888.

Oswal, A., Litvak, V., Sauleau, P., and Brown, P. (2012). Beta reactivity, prospective facilitation of executive processing, and its dependence on dopaminergic therapy in Parkinson's disease. J. Neurosci. *32*, 9909–9916.

Palva, S., and Palva, J.M. (2007). New vistas for α-frequency band oscillations. Trends Neurosci. *30*, 150–158.

Palva, S., Kulashekhar, S., Hämäläinen, M., and Palva, J.M. (2011). Localization of cortical phase and amplitude dynamics during visual working memory encoding and retention. J. Neurosci. *31*, 5013–5025.

Pesaran, B., Nelson, M.J., and Andersen, R.A. (2008). Free choice activates a decision circuit between frontal and parietal cortex. Nature *453*, 406–409.

Pfurtscheller, G. (1981). Central beta rhythm during sensorimotor activities in man. Electroencephalogr. Clin. Neurophysiol. *51*, 253–264.

Pfurtscheller, G. (2001). Functional brain imaging based on ERD/ERS. Vision Res. *41*, 1257–1260.

Rainer, G., Rao, S.C., and Miller, E.K. (1999). Prospective coding for objects in primate prefrontal cortex. J. Neurosci. *19*, 5493–5505.

Ray, W.J., and Cole, H.W. (1985). EEG alpha activity reflects attentional demands, and beta activity reflects emotional and cognitive processes. Science *228*, 750–752.

Rigotti, M., Ben Dayan Rubin, D., Wang, X.J., and Fusi, S. (2010). Internal representation of task rules by recurrent dynamics: the importance of the diversity of neural responses. Front Comput Neurosci. *4*, 24.

Rogers, R.D., and Monsell, S. (1995). Costs of a predictable switch between simple cognitive tasks. J. Exp. Psychol. Gen. *124*, 207–231.

Sadaghiani, S., Scheeringa, R., Lehongre, K., Morillon, B., Giraud, A.L., and Kleinschmidt, A. (2010). Intrinsic connectivity networks, alpha oscillations, and tonic alertness: a simultaneous electroencephalography/functional magnetic resonance imaging study. J. Neurosci. *30*, 10243–10250.

Sakai, K., and Passingham, R.E. (2003). Prefrontal interactions reflect future task operations. Nat. Neurosci. *6*, 75–81.

Sauseng, P., Klimesch, W., Stadler, W., Schabus, M., Doppelmayr, M., Hanslmayr, S., Gruber, W.R., and Birbaumer, N. (2005). A shift of visual spatial attention is selectively associated with human EEG alpha activity. Eur. J. Neurosci. *22*, 2917–2926.

Sejnowski, T.J., and Paulsen, O. (2006). Network oscillations: emerging computational principles. J. Neurosci. *26*, 1673–1676.

Siegel, M., Donner, T.H., and Engel, A.K. (2012). Spectral fingerprints of large-scale neuronal interactions. Nat. Rev. Neurosci. *13*, 121–134.

Stuss, D.T., and Benson, D.F. (1984). Neuropsychological studies of the frontal lobes. Psychol. Bull. *95*, 3–28.

Swann, N., Tandon, N., Canolty, R., Ellmore, T.M., McEvoy, L.K., Dreyer, S., DiSano, M., and Aron, A.R. (2009). Intracranial EEG reveals a time- and frequency-specific role for the right inferior frontal gyrus and primary

motor cortex in stopping initiated responses. J. Neurosci. *29*, 12675–12685.

von Stein, A., Chiang, C., and König, P. (2000). Top-down processing mediated by interareal synchronization. Proc. Natl. Acad. Sci. USA *97*, 14748–14753.

Wallis, J.D., Anderson, K.C., and Miller, E.K. (2001). Single neurons in prefrontal cortex encode abstract rules. Nature *411*, 953–956.

White, I.M., and Wise, S.P. (1999). Rule-dependent neuronal activity in the prefrontal cortex. Exp. Brain Res. *126*, 315–335.

Womelsdorf, T., Schoffelen, J.-M., Oostenveld, R., Singer, W., Desimone, R., Engel, A.K., and Fries, P. (2007). Modulation of neuronal interactions through neuronal synchronization. Science *316*, 1609–1612.

Worden, M.S., Foxe, J.J., Wang, N., and Simpson, G.V. (2000). Anticipatory biasing of visuospatial attention indexed by retinotopically specific-band electroencephalography increases over occipital cortex. J. Neurosci. *20*, RC63.

Zhang, Y., Wang, X., Bressler, S.L., Chen, Y., and Ding, M. (2008). Prestimulus cortical activity is correlated with speed of visuomotor processing. J. Cogn. Neurosci. *20*, 1915–1925.